Journal of Energy & Environment Management

Aurora Wings Publishing

Doi: https://doi.org/10.63333/eem.v1n15

Vol. 1 No. 1 (2025)

Slaking tests of soil-rock mixture and the simulation of state-dependent elastoplastic model

Hai Tian[1,*], Zhiliang Sun[2]

[1] School of Architecture Engineering, Huanggang Polytechnic College, Huanggang 438000, China;
[2] Institute of Rock and Soil Mechanics, Chine Academy of Sciences, Wuhan 430071, China.
* Correspondence: h-tien@outlook.com

Abstract: A series of large-scale triaxial tests employing the 'dual-line' methodology were performed to examine the slaking mechanical behavior of soil-rock mixture materials characterized by both dense and loose compactness. The study analyzed the impact of slaking on several parameters, including the secant modulus (E_{50}), the critical state friction angle, the peak state friction angle, and the positioning of the critical state line. The findings reveal that the slaking process leads to a reduction in the secant modulus E_{50}, as well as in both the critical state and peak state friction angles. Notable alterations in the isotropic compression line and the critical state line were observed in the soil prior to and following wetting. Subsequently, utilizing a state-dependent constitutive model for cohesionless soils, the stress-strain relationship of the deposit was simulated both before and after wetting. The results of the model simulation were found to effectively capture the changes in shear dilatancy characteristics of the deposit in relation to the wetting process, in comparison to the experimental data.

Keywords: Large-Scale Triaxial Test; Soil-Rock Mixture; Critical State; Shear Dilatancy; Constitutive Equation

1. Introduction

Soil-rock mixture slopes, prevalent in southwestern China, are primarily composed of Quaternary deposits that include various loose slope deposits, avalanche slope deposits, and alluvial deposits. These mixtures typically consist of rocks, large gravel particles, and weathered clay minerals, characterized by a particle size distribution and an unstable structure that predominantly exhibits a 'binary structure' of soil and stone. Such deposits are commonly found in slope formations across numerous reservoir areas. Hydrological factors, such as intense rainfall or fluctuations in groundwater levels, serve as critical triggers for slope failure. Effective environmental management must focus on the implementation of drainage systems and the enhancement of water retention capacity. The interplay between slope stability and environmental management is reciprocal, necessitating integrated strategies to maintain ecological balance and ensure human safety. The stability of these slopes is significantly influenced by the processes of water infiltration and the drying-wetting cycle. Slaking, defined as the alternation of wetting and drying, is particularly relevant; rocks, especially those containing clay, exhibit swelling upon wetting and subsequent contraction during drying. The infiltration of water into the pores of the rock leads to dilation, which induces tensile stresses and results in the formation of tension cracks [1, 2]. Consequently, investigating the slaking characteristics of soil-rock mixture materials and conducting

Doi: https://doi.org/10.63333/eem.v1n15 Vol. 1 No. 1 (2025)

numerical simulations are essential for engineering applications. Furthermore, soil-rock mixture materials are frequently utilized in embankment construction, and the slaking deformation of these embankments serves as a critical parameter for assessing construction quality [3-6].

The slaking behavior of soil-rock mixtures is intricate and influenced by various factors, including grading, mineral composition, confining pressure, and density [7-11]. Slaking occurs when aggregates lack the strength to endure internal stresses from rapid water absorption. These internal stresses arise from uneven swelling of clay particles, air trapped and escaping in soil pores, quick heat release during wetting, and the mechanical movement of water. [12, 13]. The impact of slaking on the mechanical properties and deformation of coarse-grained soil has been thoroughly examined through triaxial slaking tests on clay-sand mixtures. Results indicated that as water content increases, the tangent modulus of the sample decreases, while cohesion diminishes with higher slaking stress levels, although the friction angle remains relatively constant [14, 15]. Comprehensive slaking tests conducted on granite and metamorphic rockfills have demonstrated a linear correlation between volume strain and stress levels during the slaking process, while the relationship between axial strain and stress levels can be characterized by exponential functions [16, 17]. Although the shear strength of slate coarse-grained materials exhibits variations following wetting, the strength index of coarse-grained soil remains largely unaffected across different stress levels [18, 19]. The classical stress dilatancy theory has proven inadequate in formulating a cohesive constitutive model applicable to both loose and dense sand across a broad spectrum of density and stress conditions [20]. It is posited that the dilatancy of granular soil is contingent upon both the external stress state and the internal physical state, with the latter typically encompassing parameters such as compactness and confining pressure, as discussed in the existing literature [21-23]. This study employs the principles of critical state soil mechanics and utilizes a large-scale triaxial apparatus to investigate the stress-strain relationships of soil-rock mixtures before and after wetting, under conditions of both intensive and loose compactness and varying confining pressures. The research aims to analyze the impact of slaking on the mechanical properties of the soil-rock mixture by examining the physical state changes that occur pre- and post-wetting. Subsequently, the stress-strain relationship is modeled using a state-dependent elastoplastic constitutive framework, which is then validated against experimental results to assess the model's applicability.

2. Materials and Methods

2.1. Slaking of soil-rock mixture

Currently, there exist two primary methodologies for conducting slaking tests: the dual-line method and the single-line method. The ‘single-line’ method involves saturating dry soil under a specific stress state and subsequently measuring the deformation of the sample during immersion. Conversely, the ‘dual-line’ method entails the preparation of two samples of geotechnical mixed materials that share identical initial conditions. One sample is subjected to conventional triaxial testing in its natural dry state, while the other is saturated with water and tested under wetting conditions using triaxial testing. The phenomenon of slaking results in a decrease in effective stress, a weakening of the interconnections between soil particles, and an increase in pore pressure, which collectively lead to a reduction in shear strength and a decline in the deformation modulus. By comparing the outcomes of the two samples, researchers can analyze the variations in parameters such as shear strength and deformation modulus that are induced by wetting. This method is particularly noteworthy as it allows for the comparison of deformation differences under identical stress states between dry and saturated samples, thereby providing insights into the hydro-mechanical behavior of granular materials under varying moisture conditions. Although the ‘single-line’ method is often deemed more practical for wetting and is frequently recommended for various applications, its experimental execution is relatively complex [24-26]. Furthermore, when applied to calculations, the tangential modulus and tangential Poisson's ratio of the sample cannot be derived from the test data obtained through the ‘single-line’ method during wetting, and the incremental Hooke's law is not applicable for calculating immersion deformation. Additionally, the suitability of conventional triaxial tests for complex stress paths remains questionable [27]. While

Doi: https://doi.org/10.63333/eem.v1n15 Vol. 1 No. 1 (2025)

the dual-line method may not align perfectly with the actual stress and flooding paths, it is characterized by its simplicity and ease of operation. To investigate the alterations in mechanical properties of the soil-rock mixture before and after wetting, the 'dual-line' method was employed for the slaking test.

2.2. Large-scale triaxial tests

A large-scale triaxial apparatus was used in the test. The main technical parameters of the equipment: (1) maximum axial load 2500 kN, (2) maximum ambient pressure 5.0 MPa, (3) maximum back pressure 2.0 MPa and (4) axial deformation rate 0.1–30 mm/min.

The deposit used for the test was taken from a section of Mianmao Road in Deyang, Sichuan, China. The particle size distribution (PSD) of soil materials is shown in Table 1. The control of dry density affects its strength, deformation, and failure mode by changing the pore structure, particle contact state, and water-force coupling of the soil-rock mixture. In engineering, it is necessary to consider factors such as gradation and moisture content, and to determine the optimal range of dry density through experiments to achieve a balance between mechanical performance and stability. In order to study the effect of different controlled dry densities on the mechanical properties of soil-rock mixtures, the experimental subjects used two groups of soil-rock mixture samples with controlled dry densities for the triaxial slaking process (see Table 2). The sample size is Φ300 mm × H600 mm. To minimise segregation of coarse and fine particles during loading and improve the uniformity of the sample, the sample was divided into five layers, where each layer was 120 mm, and each layer is prepared according to the graded and controlled dry density. After packing, vibration is layered according to control height, air-dried samples are filled directly with air-dried materials, and saturated samples after filling with air-dried materials are vacuum-pumped and saturated with water for about 8 h to ensure that the sample is fully saturated. Twenty sets of large-scale triaxial tests were conducted in four groups. To control the influence of consolidation time on the test results, the consolidation time of each sample was controlled at about 3 h, which could ensure the stability of the sample consolidation. The experimental scheme is shown in Table 3.

Table 1. Particle size distribution of tested deposit

Grain size (mm)						
60-40	**40-20**	**20-10**	**10-5**	**5-2**	**2-1**	**＜1**
14.2	28.7	26.8	12.4	17.9	10.8	6.5

Table 2. Physical properties of soil-rock mixture

G_s (*Specific gravity*)	d_{50} (*Average grain size*) mm	C_u (*Nonuniformity coefficient*)	C_c (*curvature coefficient*)	ρ_{dmax} (*Maximum dry density*) g·cm^{-3}	ρ_{dmin} (*Minimum dry density*) g·cm^{-3}
2.657	17.3	11.6	2.46	2.379	1.419

Table 3. Scheme of large-scale triaxial tests with respect to soil-rock mixture

Test type	ρ_d (*dry density*) (g·cm^{-3})	σ_3 (*Confining pressure*) (kPa)	**Shear rate** (mm/min)
Consolidation-drained (Saturated sample)	2.14 1.90 2.14	200、400、600、800、1000	0.6

Doi: https://doi.org/10.63333/eem.v1n15 Vol. 1 No. 1 (2025)

Consolidation-drained (Dry sample)	1.90

2.3. Slaking on friction angle

The critical state is an ideal limit state in which the deviatoric stress and mass variation of soil mass do not change during continuous deformation, but it is difficult to reach this state due to the limitations of axial displacement range of the triaxial test system. The critical friction angle is speculated according to the method proposed by Indraratna et al. [28]. The relationship between friction angle and confining pressure of the deposit under various working conditions can be expressed as

$$\varphi_c = \varphi_{c0} - \Delta\varphi_c \ln(p_0/p_a) \quad (2.1)$$

$$\varphi_p = \varphi_{p0} - \Delta\varphi_p \ln(p_0/p_a) \quad (2.2)$$

where p_0 is the initial average effective stress, p_a is the atmospheric pressure (100 kPa), φ_{c0} and φ_{p0} are the critical and peak state friction angles, respectively.

According to the critical state soil mechanics theory, the sliding friction angle under triaxial compression can be defined as

$$\sin\varphi_m = \frac{3\eta}{6+\eta} \quad (2.3)$$

where φ_m is friction angle, $\eta=q/p'$ is the stress ratio, and, therefore, the critical state friction angle φ_c can be defined as

$$\sin\varphi_c = \frac{3M_c}{6+M_c} \quad (2.4)$$

where M_c is the critical state stress ratio. By substituting Equation (2.1) into Equation (2.4), the critical state stress ratio under different initial effective stress conditions can be obtained as follows:

$$M_c = \frac{6\sin[\varphi_{c0}-\Delta\varphi_c \ln(p_0/p_a)]}{3-\sin[\varphi_{c0}-\Delta\varphi_c \ln(p_0/p_a)]} \quad (2.5)$$

The isotropic consolidation curve at low confining pressure before and after wetting can be simplified as

$$e_i = e_{i0} - \lambda_i \ln(p'/p_a) \quad (2.6)$$

where e_i is the void ratio of isotropic consolidation state, p' *is* the average effective stress, p_a is atmospheric pressure (100kPa), e_{i0} is void ratio in the isotropic consolidation state, λ_i is the slope of the ICL (isotropic compression line) in the plane of e–lnp'.

After the shear reaches its critical state, the critical state line (CSL) in the e–lnp' space can be expressed as

$$e_c = e_{c0} - \lambda_c \ln(p'/p_a) \quad (2.7)$$

where e_c is the critical state void ratio, e_{c0} is the critical state void ratio when $p' = p_a$, λ_c is the slope of the CSL (critical state line) in the plane of e–ln$p$.

2.4. State-dependent elastoplastic constitutive model

The stress-strain relationship of soil-rock mixtures exhibits significant nonlinearity and dilatancy characteristics due to the interlocking effect between particles and the friction at the soil-rock interface. State-dependent elastoplastic models can describe the degradation of stiffness and volume change characteristics of the material during the transition from the elastic to the plastic stage by introducing critical state theory (such as the hardening rules of the modified Cambridge model) and related flow rules.

In addition, the mechanical properties of soil-rock mixtures are significantly influenced by the characteristics of the interface between rock blocks and soil, as well as the particle gradation. State-dependent models reflect the gradual failure process of the material through stiffness degradation mechanisms, and their analytical results are closer to the structural responses observed in actual engineering compared to elastic models.

Doi: https://doi.org/10.63333/eem.v1n15 Vol. 1 No. 1 (2025)

In summary, state-dependent elastoplastic constitutive models have the potential to describe the mechanical behaviour of soil-rock mixtures within a theoretical framework, balancing theoretical innovation and engineering practicality in their application to soil-rock mixtures.

In elastic–plastic theory, the flow law is closely related to the dilatancy ratio d_r, which is usually defined as the ratio of plastic volumetric strain increment ($d\varepsilon_v^p$) to plastic deviator strain increment ($d\varepsilon_s^p$), and thus $d_r = d\varepsilon_v^p / d\varepsilon_s^p$. Been et al. [29], on the basis of criticality theory, proposed to use state parameters (ψ) to reflect the degree of looseness of granular materials. ψ is defined as the difference between the current void ratio (e) and critical void ratio (e_c) under the same corresponding pressure, that is

$$\psi = e - e_c \tag{2.8}$$

Incorporating (2.7) into (2.8), state parameters (ψ) can be represented as

$$\psi = e - e_{c0} + \lambda_c \ln(p'/p_a) \tag{2.9}$$

The dilatancy equation proposed by Li et al. [20, 30, 31] is

$$d_r = \frac{d\varepsilon_v^p}{d\varepsilon_s^p} = \frac{d_0}{M_C}(M_d - \eta) \tag{2.10}$$

where $M_d = M_c \cdot \exp(k_d \psi)$, which can then be substituted into Equation (2.10) to obtain the state-related dilatancy equation.

$$d_r = \frac{d_0}{M_C}\left\{M_c \exp\left[k_d\left(e - e_{c0} + \lambda_c \ln(p'/p_a)\right)\right] - \eta\right\} \tag{2.11}$$

In this equation, M_c represents the critical state stress ratio, M_d represents the dilatancy stress ratio and d_0 and k_d are the material-related constants. Li et al. [20] also proposed a simplified yield surface equation and assumed that when the stress ratio (η) exceeds its historical maximum stress, plastic strain will start to occur, while the path of equal stress ratio will not produce plastic strain, and η is the hardening criterion. This assumption is applicable to the conventional triaxial compression stress path, and the simplified yield surface equation is

$$f = q - \eta_s p' = 0 \tag{2.12}$$

The stress–strain relationship of elastoplastic in the incremental form can be expressed as

$$\dot{\boldsymbol{\sigma}} = \left\{\mathbf{D}^e - \frac{\mathbf{D}^e \mathbf{m}\mathbf{n}^T \mathbf{D}^e}{H_p + \mathbf{n}^T \mathbf{D}^e \mathbf{m}}\right\} \dot{\boldsymbol{\varepsilon}} \tag{2.13}$$

where $\mathbf{D}^e$ is the elastic modulus matrix, $\mathbf{m} = [n_v^g, n_s^g]^T$ is the unit vector of plastic flow direction and $\mathbf{n} = [n_v^f, n_s^f]^T$ is the unit hardening vector perpendicular to the loading surface of the current stress state.

According to Equation (2.12), the hardening direction (n_v^f, n_s^f) in p'–q space is

$$n_v^f = \frac{1}{L_f}\frac{\partial f}{\partial p'} = \frac{-\eta}{\sqrt{1+\eta^2}} \tag{2.14}$$

$$n_s^f = \frac{1}{L_f}\frac{\partial f}{\partial q} = \frac{1}{\sqrt{1+\eta^2}} \tag{2.15}$$

The plastic flow direction (n_v^g, n_s^g) is

$$n_v^g = \frac{1}{L_g}\frac{\partial g}{\partial p'} = \frac{d}{\sqrt{1+d^2}} \tag{2.16}$$

$$n_s^g = \frac{1}{L_g}\frac{\partial g}{\partial q} = \frac{1}{\sqrt{1+d^2}} \tag{2.17}$$

According to the uncorrelated flow law, the plastic strain increment ($d\varepsilon_v^p$, $d\varepsilon_s^p$) can be expressed as

$$d\varepsilon_v^p = \frac{\left(n_v^f dp' + n_s^f dq\right) n_v^g}{H_p} \tag{2.18}$$

$$d\varepsilon_s^p = \frac{\left(n_v^f dp' + n_q^f dq\right) n_s^g}{H_p} \tag{2.19}$$

Where H_p is the plastic modulus, and the elastic part of the strain is

$$d\varepsilon_s^e = \frac{dq}{3G} \tag{2.20}$$

$$d\varepsilon_v^e = \frac{dp'}{K} \tag{2.21}$$

Doi: https://doi.org/10.63333/eem.v1n15 Vol. 1 No. 1 (2025)

$$\begin{pmatrix} \mathrm{d}q \\ \mathrm{d}p' \end{pmatrix} = \begin{bmatrix} \begin{pmatrix} 3G & 0 \\ 0 & K \end{pmatrix} \\ \frac{\langle L \rangle}{H_\mathrm{p}+3G-K\eta d} \quad \begin{pmatrix} 9G^2 & -3KG\eta \\ 3KGd & -K^2\eta d \end{pmatrix} \end{bmatrix} \begin{pmatrix} \mathrm{d}\varepsilon_\mathrm{s} \\ \mathrm{d}\varepsilon_\mathrm{v} \end{pmatrix} \tag{2.22}$$

In equation (2.22) when $L > 0$, $\langle L \rangle = 1$, but in all other cases, $\langle L \rangle = 0$. G and K are the elastic shear modulus and the elastic volume modulus, respectively, which can be expressed as

$$G = G_0 \frac{(2.17-e)^2}{(1+e)} \sqrt{p_a p'} \tag{2.23}$$

$$K = G \frac{2(1+\mu)}{3(1-2\mu)} \tag{2.24}$$

where G_0 is the material parameter, μ is Poisson's ratio and e is the current porosity ratio. Li et al. [20] proposed a simplified form:

$$H_\mathrm{p} = hG \left[\frac{M_c}{\eta} - \exp\left(k_p \psi\right) \right] \tag{2.25}$$

where, h and k_p are model parameters, M_c is a function of the initial mean effective stress p_0, which is represented by φ_c and $\Delta\varphi_\mathrm{c}$ according to (2.5). In summary, the simplified state-dependent constitutive model involves 10 model parameters: $\varphi_{\mathrm{c}0}$, $\Delta\varphi_\mathrm{c}$, $e_{\mathrm{c}0}$, λ_c, d_0, k_d, k_p, h, G_0 and μ.

2.5. Simulation parameters based on state-dependent constitutive modelling

For large triaxial consolidation drainage tests, the stress–strain relationship is as follows:

$$\mathrm{d}q = 3\mathrm{d}p' \tag{2.26}$$

$$\mathrm{d}\varepsilon_\mathrm{v} = \mathrm{d}\varepsilon_a + 2\mathrm{d}\varepsilon_r \tag{2.27}$$

$$\mathrm{d}\varepsilon_q = \frac{2}{3}(\mathrm{d}\varepsilon_a - \mathrm{d}\varepsilon_r) \tag{2.28}$$

Substituting Equations (2.26), (2.27) and (2.28) into Equation (2.22), the increment of partial stress ($\mathrm{d}q$) and the increment of average effective stress ($\mathrm{d}p'$) can be obtained according to the axial strain increment (ε_a).

Compared with the saturated deposit before and after wetting, the stress–strain relationship of the air-dried deposit has little effect on M_c, λ_c and the form of dilatancy equation, or, in other words, the critical state parameters and the state-related parameters do not change before and after wetting. Considering the influence of different initial water contents on $e_{\mathrm{c}0}$ and G_0, the same set of parameters can be used to describe the slaking stress–strain relationship of the deposit by the double-line method. The influence of slaking on $e_{\mathrm{c}0}$ is mainly to ensure $e_{\mathrm{c}0\text{-d}}$ in the corresponding air-dried state moves downward to $e_{\mathrm{c}0\text{-w}}$-W in the slaking saturation state, which can be expressed as $e_{\mathrm{c}0\text{-w}} = e_{\mathrm{c}0\text{-d}} - \Delta e$. The softening effect of slaking on the elastic modulus is mainly considered by the reduction coefficient (β), that is $G_{0\text{-w}} = \beta G_{0\text{-d}}$.

3. Results and Discussion

3.1. Test results

Figure 1 illustrates the stress-strain curve associated with large-scale triaxial slaking of a soil-rock mixture, as analyzed through the 'dual-line' method. The findings indicate that the air-dried deposits, subjected to the specified grading, exhibit pronounced characteristics of strain softening and dilatancy throughout the shearing process. Notably, under identical confining pressures, the dilatancy observed in the sample with a dry density of ρ_d = 2.14 g·cm^{-3} (D_r = 0.836) is significantly more pronounced than that of the sample with a dry density of 1.90 g·cm^{-3} (D_r = 0.628). Furthermore, at a constant dry density, it is evident that dilatancy increases with a reduction in confining pressure. For samples sharing the same grading and dry density, the stress-strain relationships exhibit marked differences post-saturation. For instance, at a confining pressure of σ_3 = 1000 kPa and a dry density of ρ_d = 1.90 g·cm^{-3}, the stress-strain relationship of air-dried samples demonstrates a strain softening behavior, whereas, upon dilation, the relationship transitions to a strain hardening and volume shear behavior. These observations underscore the significant impact of slaking on the mechanical properties of soil-rock mixtures.

Doi: https://doi.org/10.63333/eem.v1n15
Vol. 1 No. 1 (2025)

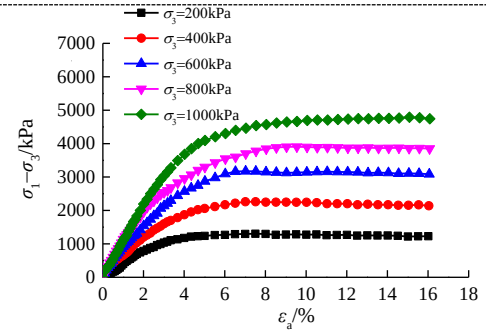

(a) Dry state, ρ_d = 2.14 g·cm^{-3}, ε_a ~ (σ_1 — σ_3) curve.

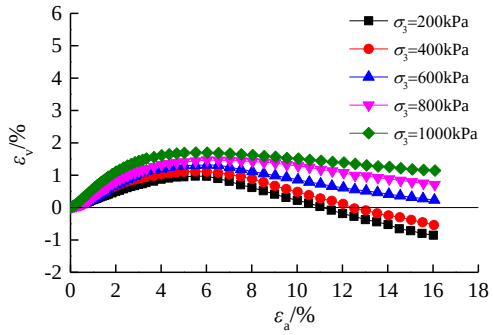

(b) Dry state, ρ_d = 2.14 g·cm^{-3}, ε_a ~ ε_v curve

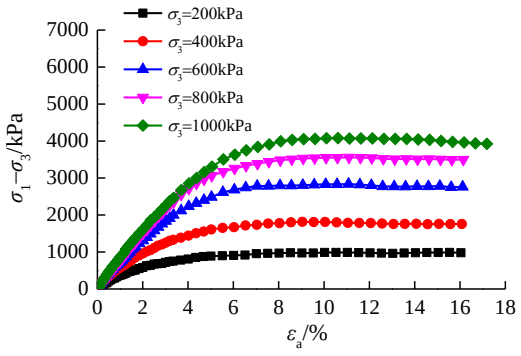

(c) Dry state, ρ_d = 1.90 g·cm^{-3}, ε_a ~ (σ_1 — σ_3) curve

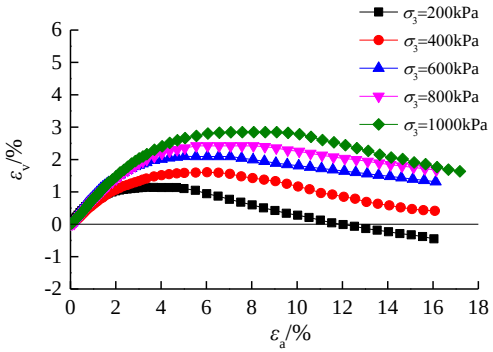

(d) Dry state, ρ_d = 1.90 g·cm^{-3}, ε_a ~ ε_v curve

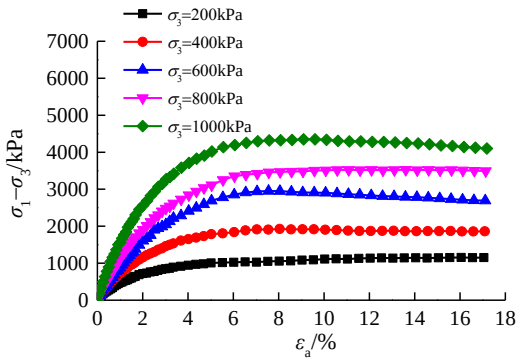

(e) Wet state, ρ_d = 2.14 g·cm^{-3}, ε_a ~ (σ_1 — σ_3) curve

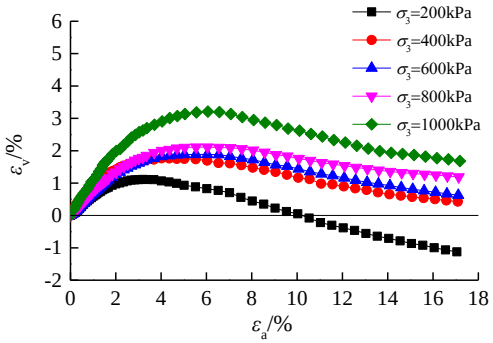

(f) Wet state, ρ_d = 2.14 g·cm^{-3}, ε_a ~ ε_v curve

Doi: https://doi.org/10.63333/eem.v1n15 Vol. 1 No. 1 (2025)

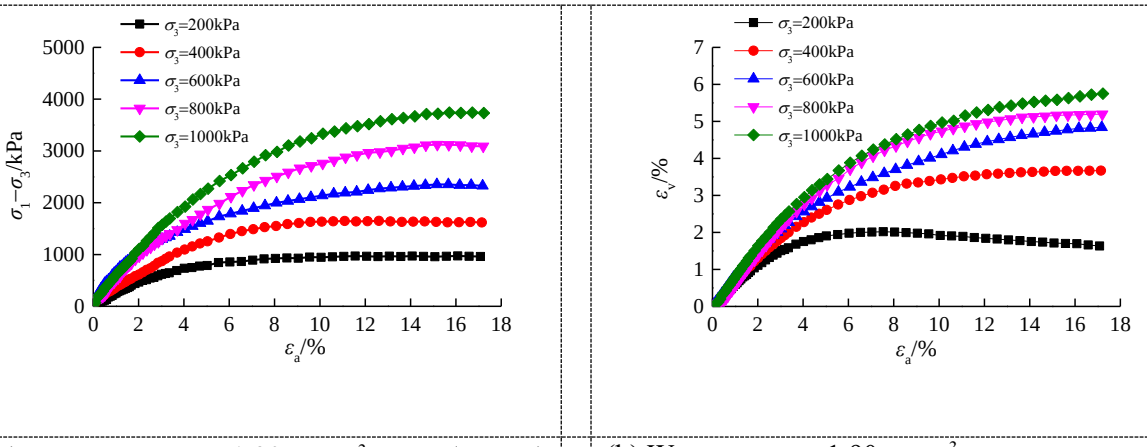

(g) Wet state, ρ_d = 1.90 g·cm^{-3}, ε_a ~ (σ_1 − σ_3) curve

(h) Wet state, ρ_d = 1.90 g·cm^{-3}, ε_a ~ ε_v curve

Figure 1. Stress–strain relationship in slaking tests on soil-rock mixture

3.2. Influence of slaking on the secant modulus of the deposit

E_{50} is characterized as the secant modulus corresponding to the point at which the stress-strain curve reaches 50% of its peak value. Mathematically, this is expressed as $E_{50} = 0.5q_p/\varepsilon_{q50}$, where qp represents the peak deviatoric stress and ε_{q50} denotes the strain value associated with q_p at the 50% mark. The correlation between the secant modulus E_{50} and the initial average effective stress p_0 across various operational conditions is illustrated in Figure 2.

As depicted in Figure 2, there is a positive correlation between the secant modulus and the initial average effective stress, indicating that E_{50} increases with higher values of p_0. Additionally, the phenomenon of slaking exerts a detrimental influence on the secant modulus. Specifically, while the reduction in E_{50} due to slaking is minimal at a dry density (ρ_d) of 2.14 g·cm^{-3}, it becomes significantly pronounced at a ρ_d of 1.90 g·cm^{-3}. For instance, at an initial average effective stress of 1000 kPa and a dry density of 1.90 g·cm^{-3}, the secant modulus of the air-dried specimen is measured at 78.8 MPa. In contrast, the corresponding sample in a saturated slaking condition exhibits a secant modulus of 50.4 MPa, reflecting a decrease of 36%.

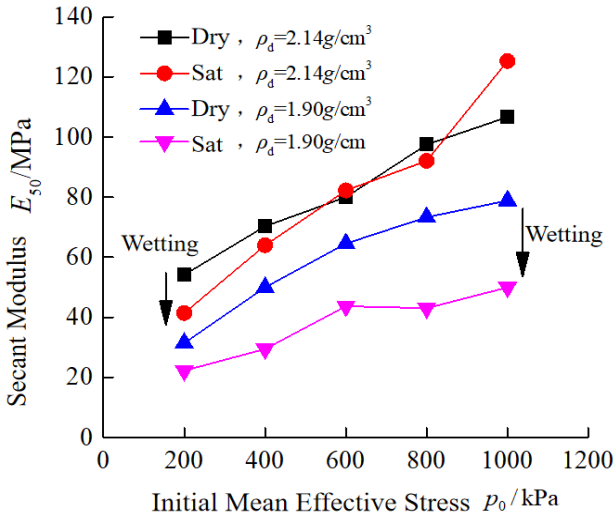

Figure 2. Relationship between secant modulus E_{50} and initial mean effective stress p_0 at various conditions.

Doi: https://doi.org/10.63333/eem.v1n15 Vol. 1 No. 1 (2025)

3.3. Effect of slaking on friction angle

The relationship between peak friction angle and confining pressure before and after wetting is shown in Figure 3, and the critical state points are plotted on the graph for comparison. It can be seen from the Figure 3 that the variation trend of friction angle in the peak state with confining pressure is basically the same as that in its critical state. The peak friction angle and the critical state friction angle of the deposit are closely related to the initial confining pressure and decrease with increasing confining pressure, which presents obvious stress correlation and nonlinear characteristics. C*u* and $\Delta\varphi_p$ are fitting parameters, and detailed parameter values are shown in Table 4.

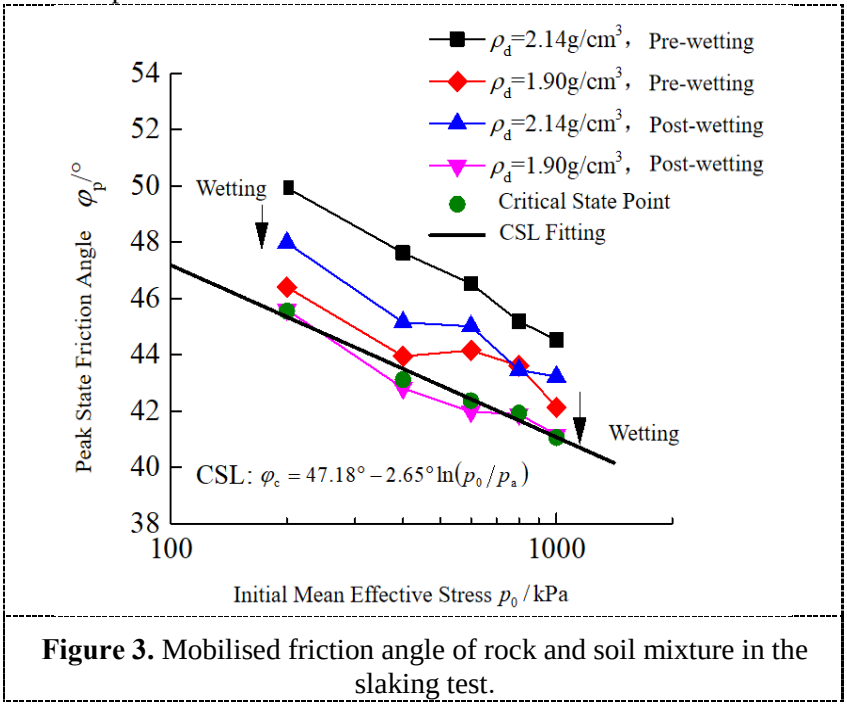

Figure 3. Mobilised friction angle of rock and soil mixture in the slaking test.

Table 4. Fitting parameters of $\varphi_c - \ln(p_0/p_a)$ and $\varphi_p - \ln(p_0/p_a)$

Slaking state	Critical state		Peak state	
	φ_{c0} /°	$\Delta\varphi_c$ /°	φ_{p0} /°	$\Delta\varphi_p$ /°
ρ_d=2.14 g·cm^{-3}. Before wetting	47.18	2.65	52.14	3.02
ρ_d=2.14 g·cm^{-3}. After wetting			49.77	2.71
ρ_d=1.90 g·cm^{-3}. Before wetting			47.77	2.25
ρ_d=1.90 g·cm^{-3}. After wetting			47.04	2.64

3.4. Influence of slaking on the state line of the deposit

Figure 4 shows the *p'*–*e* relationship before and after wetting in the *p'*–*e* projection plane. The fitting lines of ICL and CSL in the plane of *e*–ln*p'* are basically parallel before and after wetting; therefore, the fitting parameters λ_i and λ_c can have the same value before and after wetting, and the specific fitting parameters are shown in Table 5. It should be pointed out that the slope of the CSL of the deposit with a density of 2.14 g·cm^{-3} (D_r = 0.836) is different from that with a density of 1.90 g·cm^{-3} (D_r = 0.628) in the plane of the *e*–ln*p'* projection plane. This is different from the view held by Xiao et al. [22, 32] that the slope of the CSL of rockfill material with different densities is basically the same. This may be because the fine particle content of the deposit in this test is higher.

Doi: https://doi.org/10.63333/eem.v1n15 Vol. 1 No. 1 (2025)

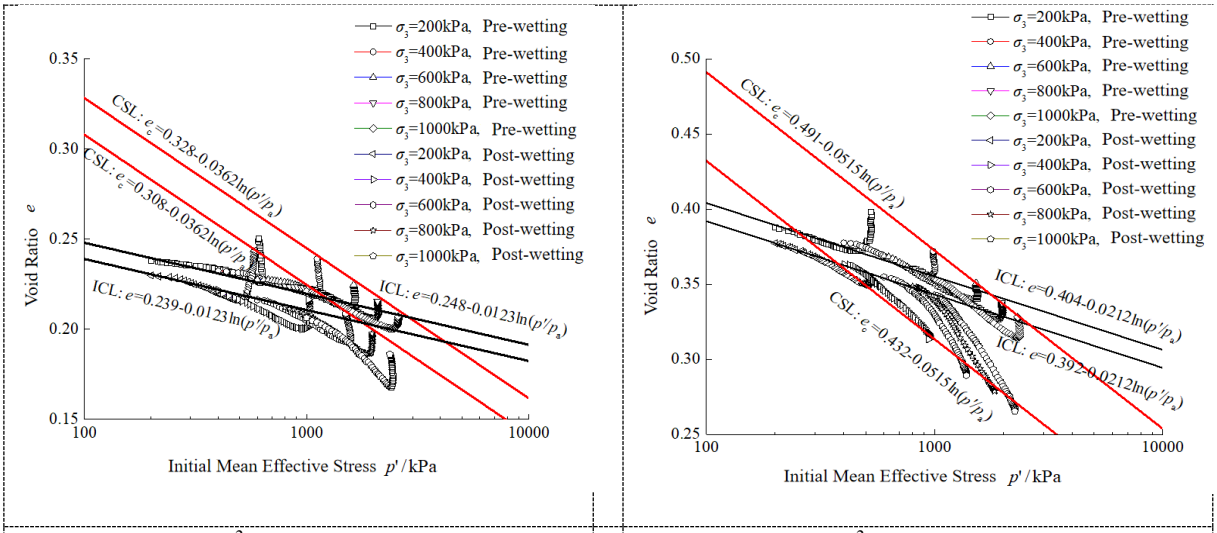

(a) ρ_d = 2.14 g·cm^{-3} (b) ρ_d = 1.90 g·cm^{-3}

Figure 4. State lines of soil-rock mixture on the *e* - ln*p*' projective plane

Table 5. Fitting parameters of ICL and CSL

Slaking state	Fitting parameters of ICL		Fitting parameters of CSL	
	λ_i	e_{i0}	λ_c	e_{c0}
2.14 g·cm^{-3}. Before wetting	0.0123	0.248	0.0362	0.328
2.14 g·cm^{-3}. After wetting		0.239		0.308
1.90 g·cm^{-3}. Before wetting	0.0212	0.404	0.0515	0.491
1.90 g·cm^{-3}. After wetting		0.392		0.432

3.5. Simulation results

According to the experimental results in Figure 2, when the dry density of the deposit is 2.14 g·cm^{-3}, Δe = 0.020 and β = 0.967 and when ρ_d = 1.90 g·cm^{-3}, Δe = 0.059 and β = 0.613. Other model parameters can be seen in Table 6.

Table 6. Model parameters of soil-rock mixture

Elastic parameter	Critical state parameter	Parameters related state	Parameters influencing slaking
G_0 = 124 ν = 0.32	φ_{c0} = 47.18	d_0 = 2.32	ρ_d = 2.14 g·cm^{-3}, β = 0.967, Δe = 0.020;
	$\Delta\varphi_c$ = 2.65	k_d = 1.09	
	λ_c = 0.0362	k_p = 2.15	ρ_d = 1.90 g·cm^{-3}, β = 0.613, Δe =0.059
	e_{c0} = 0.328	h = 0.85	

Figure 5 presents a comparative analysis of simulation outcomes and empirical results pertaining to the state-dependent constitutive model. The model demonstrates superior predictive capabilities regarding the triaxial loading stress-strain relationship of soil-rock mixtures, encompassing both strain hardening accompanied by shear shrinkage and strain softening associated with dilatancy. This indicates that the proposed state-dependent constitutive model exhibits a high degree of adaptability to triaxial

Doi: https://doi.org/10.63333/eem.v1n15 Vol. 1 No. 1 (2025)

testing conditions and effectively characterizes the internal state of the soil-rock mixture, the effective consolidation pressure, and the impact of slaking on its stress-strain behavior.

Furthermore, it is evident from Figure 5 that the model's performance on the ε_a~(σ_1-σ_3) curve is generally more favorable than that on the ε_a~ε_v curve. This discrepancy may be attributed to several factors, including the substantial volume of the sample, the loading rate, and the ambient temperature during testing. Additionally, the air-dry exhaust test was conducted using a U-tube, whereas the saturation Consolidated-Drained test utilized a volumetric variable tube, which is intricately linked to the drainage of pore water within the sample. These factors may significantly influence the ε_a~ε_v curve. Overall, the enhanced state-dependent constitutive model effectively captures the changes in dilatancy of the deposit before and after wetting.

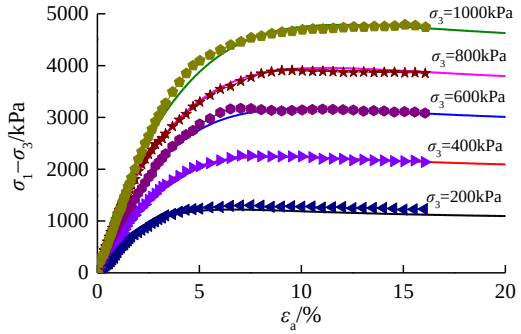

(a) Dry state, ρ_d = 2.14 g·cm^{-3}, ε_a ~ (σ_1 — σ_3) curve.

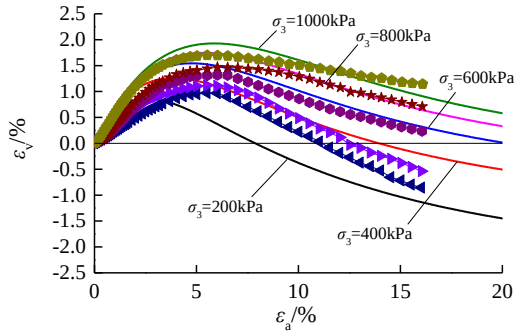

(b) Dry state, ρ_d = 2.14 g·cm^{-3}, ε_a ~ ε_v curve

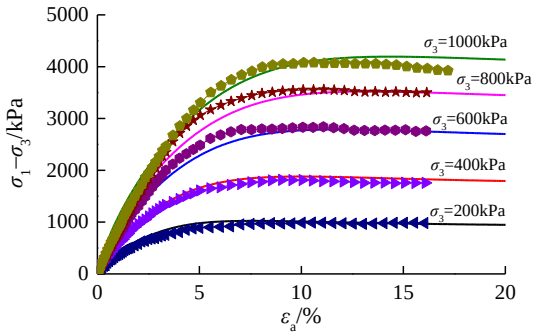

(c) Dry state, ρ_d = 1.90 g·cm^{-3}, ε_a ~ (σ_1 — σ_3) curve

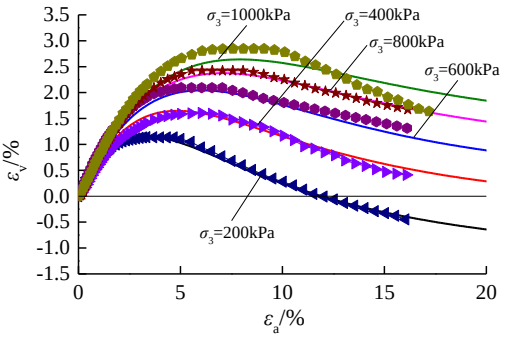

(d) Dry state, ρ_d = 1.90 g·cm^{-3}, ε_a ~ ε_v curve

Doi: https://doi.org/10.63333/eem.v1n15 Vol. 1 No. 1 (2025)

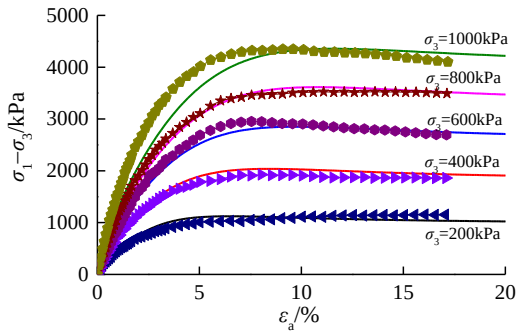

(e) Wet state, ρ_d = 2.14 g·cm^{-3}, $\varepsilon_a \sim (\sigma_1 - \sigma_3)$ curve

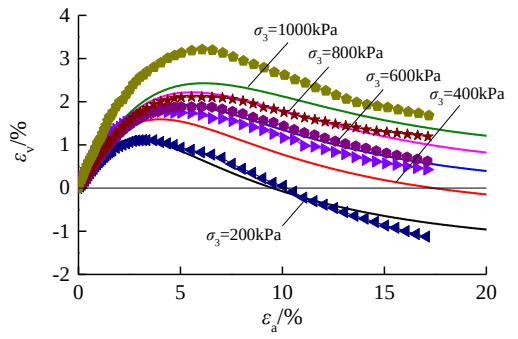

(f) Wet state, ρ_d = 2.14 g·cm^{-3}, $\varepsilon_a \sim \varepsilon_v$ curve

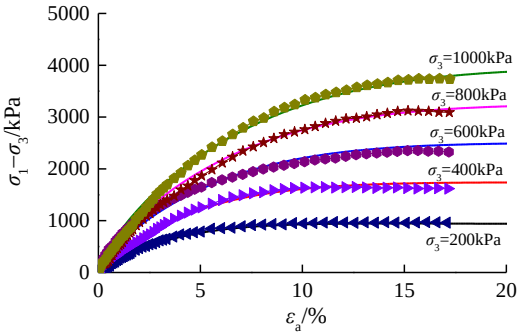

(g) Wet state, ρ_d = 1.90 g·cm^{-3}, $\varepsilon_a \sim (\sigma_1 - \sigma_3)$ curve

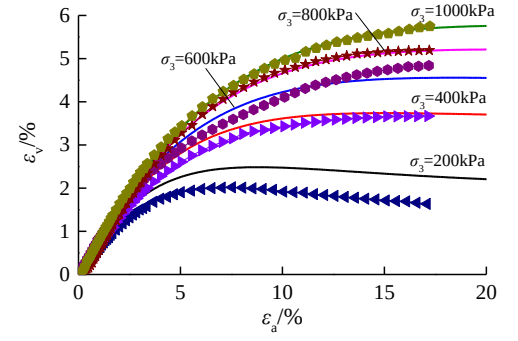

(h) Wet state, ρ_d = 1.90 g·cm^{-3}, $\varepsilon_a \sim \varepsilon_v$ curve

Figure 5. Comparison between simulation and test results of the relationship between stress and strain in slaking tests

4. Conclusion

Contemporary methodologies such as geotechnical modeling and slope stability analysis are instrumental in forecasting failure risks, thereby informing land-use planning and development regulations. Effective environmental management plays a crucial role in enhancing slope stability by preserving natural buffers, while stable slopes contribute to the maintenance of ecosystems and the mitigation of sedimentation in aquatic environments. The relationship between the friction angle and initial effective stress of a soil-rock mixture, both prior to and following wetting, can be articulated through the equation $\varphi = \varphi_0 - \Delta\varphi \ln(p_0/p_a)$. This equation indicates that the friction angle of the deposit diminishes as the initial effective stress increases, with strength parameters exhibiting notable stress correlation and nonlinear characteristics.

Slaking exerts a detrimental influence on the secant modulus (E_{50}) and the peak state friction angle of the soil-rock mixture. The weakening effect becomes more pronounced as the dry density decreases. Notably, the slope of the critical state line (CSL) for a sample with a dry density of 2.14 g/cm³ (D_r = 0.836) diverges from that of a sample with a dry density of 1.90 g/cm³ (D_r = 0.628), which in turn differs from that of rockfill with a lower fine particle content.

Doi: https://doi.org/10.63333/eem.v1n15 Vol. 1 No. 1 (2025)

A comprehensive analysis of the slaking stress-strain relationship of the deposit reveals a strong fitting effect when characterizing the stress-strain relationship in both the air-dried state and its slaking saturation state within the theoretical framework of state-dependent constitutive modeling. These findings suggest that it is viable to represent the stress-strain relationship of air-dried bulk and its slaking saturation state using a consistent set of parameters.

Acknowledgments
This work was joint supported by Hubei Provincial Natural Science Foundation and Huanggang Innovation & Development of China (Project No. 2025AFD01092)

Conflict of Interest
The authors wish to confirm that there are no known conflicts of interest associated with this publication.

Data Availability
Previously reported electronic data in figures were used to support this study and are available in the paper.

References

[1] Yatsu, E. (1988) The Nature of Weathering: An Introduction. Sozosha, Tokyo., 624 pp.
[2] Herrick, J., Whitford, W., de Soyza, A., Van Zee, J., Havstad, K., Seybold, C., and Walton, M. (2001) Field soil aggregate stability kit for soil quality and rangeland health evaluations. Catena., 44(1), 27-35.
[3] Cetin, H., Lama, M., and Ertunç, A. (2000) Settlement and slaking problems in the world's fourth largest rock-fill dam, the Ataturk Dam in Turkey. Eng. Geol., 56(3-4), 225–242.
[4] Perry, E.F., and Andrews D.E. (1987) Slaking Modes of Geologic Materials and Their Impacton Embankment Stabilization. Transport. Res. Rec.: Eng. Geol., 873, 22-28.
[5] Nakano, M., and Sakai, T. (2016) Interpretation of slaking of a mudstone embankment using soil skeleton structure model concept and reproduction of embankment failure by seismic analysis. Japanese Geotechnical Society Special Publication., 2(5), 282–287.
[6] Zhou, X, Chi, S, Wang, M, Jia, Y. (2020) Study on wetting deformation characteristics of coarse granular materials and its simulation in core-wall rockfill dams. Int. J. Numer. Anal. Methods Geomech., 44: 851-873.
[7] Kikumoto, M., Putra, A.D., and Fukuda T. (2016) Slaking and deformation behaviour. Géotechnique., 66(9), 771–785.
[8] Gautam, T. and Shakoor, (2013) A. Slaking behavior of clay-bearing rocks during a one-year exposure to natural climatic conditions. Eng. Geol., 166, 17-25.
[9] Sakai, T., and Nakano, M. (2019) Effects of slaking and degree of compaction on the mechanical properties of mudstones with varying slaking properties. Soils Found., 59, 56-66.
[10] Shen, P., Tang, H., Huang, L., and Wang, D. (2018) Experimental study of slaking properties of red-bed mudstones from the Three Gorges Reservoir area. Mar. Georesour. Geotech., 37(8), 1-11.
[11] Sharma, K., Kiyota, T., and Kyokawa, H. (2017) Effect of slaking on direct shear behaviour of crushed mudstones. Soils Found., 57(2), 288-300.
[12] Noburo, H., and Katsuya, N. (2008) Breakdown process of aggregates with non-swelling and swelling clays as affected by electrolyte concentration and air condition. Clay Sci., 14(1): 33-42.
[13] Zaher, H., and Caron, J. (2008) Aggregate slaking during rapid wetting: Hydrophobicity and pore occlusion. Can. J. Soil Sci., 88(1), 85–97.
[14] Zuo, Y.M., and Shen, Z.J. (1989) Determination of deformation character of gravel sand due to wetting. Nanjing Hydraulic Research Institute: Hydro-Sci. Eng., 1: 107–113 (in Chinese).
[15] Lee, S.-K., and Park, H.-D. (2014) Comparison of observation and laboratory slaking tests in the

Doi: https://doi.org/10.63333/eem.v1n15 Vol. 1 No. 1 (2025)

assessment of coastal erosion in Cheju Island, Korea. Geosys. Eng., 17(2), 136-141.
[16] Cheng, Z, Zuo, Y., Ding, H., et al. (2010) Wetting characteristics of coarse-grained materials. Chin. J. Geotech. Eng., 32(2): 243–247. (in Chinese).
[17] Jia, Y., Xu, B., Desai, C.S., Chi, S. and Xiang B. (2020) Rockfill Particle Breakage Generated by Wetting Deformation under the Complex Stress Path. Inter. J. Geomech., 20(10), 04020166.
[18] Zhu, J., Alsakran, M.A., Gong, X., et al. (2013) Triaxial test on wetting deformation behaviour of a slate rockfill material. Chin. J. Geotech. Eng., 35(1): 170–174 (in Chinese).
[19] Al-Maamori, H.M.S., El Naggar, M.H., and Micic, S. (2019) Wetting effects and strength degradation of swelling shale evaluated from multistage triaxial test. Underground Space, 4(2), 79–97.
[20] Li, X.S., and Dafalias, Y.F. (2000) Dilatancy for cohesionless soils. Géotechnique., 50(4), 449-460.
[21] Cai, Z., Ding S., and Bi, Q. (2009) Numerical simulation of strength and deformation characters of rockfill. Chin. J. Rock. Mech. Eng., 28(7): 1327–1334 (in Chinese).
[22] Xiao, Y., Liu, H., Chen, Y., and Jiang, J. (2014) Strength and Deformation of Rockfill Material Based on Large-Scale Triaxial Compression Tests. I: Influences of Density and Pressure. J. Geotech. Geoenviron. Eng., 140(12), 04014070.
[23] Yan, W.M., and Li, X.S. (2012) Mechanical response of a medium-fine-grained decomposed granite in Hong Kong. Eng. Geol., 129–130: 1–8.
[24] Li, G.X. (1990) Experimental study and mathematic simulation on wetting behaviour of rockfill. Chin. J. Geotech. Eng., 12(5): 198–205 (in Chinese).
[25] Xiao, Y., Liu, H., Zhang, W., Liu, H., Yin, F., and Wang, Y. (2016) Testing and modeling of rockfill materials: A review. J. Rock Mech. Geotech. Eng., 8(3), 415–422.
[26] Yin, Y., Wu, Y., Zhang, B., Ding, Y., and Sun, X. (2019) Two-Stage Wetting Deformation Behaviour of Rockfill Material. Environ. Geotech., 1–16.
[27] Shen, G., Yin, Z.Z. (2009) Improvement of wetting deformation analysis method of coarse-grained materials. Chin. J. Rock Mech. Eng., 28(12): 2437–2444 (in Chinese).
[28] Indraratna, B., Nimbalkar, S., Coop, M., and Sloan, S.W. (2014) A constitutive model for coal-fouled ballast capturing the effects of particle degradation. Comp. Geotech., 61, 96–107.
[29] Been, K., and Jefferies, M.G. (1985) A state parameter for sands. Géotechnique, 35(2), 99–112.
[30] Li, X.S., and Wang, Y. (1998) Linear Representation of Steady-State Line for Sand. J. Geotech. Geoenviron. Eng., 124(12), 1215–1217.
[31] Li, X.S. (2002) A sand model with state-dependent dilatancy. Géotechnique., 52(3), 173-186.
[32] Xiao, Y., Liu, H., Chen, Y., Jiang, J., and Zhang, W. (2015) State-Dependent Constitutive Model for Rockfill Materials. Int. J. Geomech., 15(5), 04014075.